14th International Conference on Structural Safety and Reliability - ICOSSAR'25
1-6 June, 2025 - Los Angeles California, USA
R. Ghanem, E. Johnson, S. Masri and A. Olivier (Eds)

SEISMIC FRAGILITY ANALYSIS OF STEEL MOMENT RESISTING FRAME WITH MASONRY INFILL WALLS

MAO LI[1], YONG LI[2]

Department of Civil & Environmental Engineering, University of Alberta
Edmonton, Alberta, Canada T6H2G7
[1] Mao13@ualberta.ca, [2] Yong9@ualberta.ca

Key words: Probabilistic seismic hazard analysis, seismic fragility analysis, steel moment resisting frame, masonry infill wall, multiple stripe analysis

Abstract: This study presents a seismic fragility analysis of steel moment-resisting frames (SMRFs), with and without the inclusion of masonry infill walls (MIWs). Recognizing the often-overlooked structural contributions of MIWs, the analysis incorporates a detailed probabilistic seismic hazard analysis (PSHA) to generate tectonic-based ground motion sets for various hazard levels, considering dynamic properties of structures and site-specific characteristics. A 4-story SMRF building is designed and modeled in OpenSeesPy with and without MIWs. A total of 1,500 nonlinear time-history analyses (NLTHAs) are performed across 15 hazard levels, and structural demands are evaluated in terms of inter-story drift ratio (IDR). Fragility functions are developed for three performance levels. The results reveal that MIWs significantly reduce IDR with average reductions of up to 55%. Moreover, the inclusion of MIWs greatly improves fragility performance, lowering the probability of exceeding critical performance levels.

1 INTRODUCTION

Masonry infill walls (MIWs) are traditionally regarded as non-structural components which are often integrated into steel moment-resisting frame (SMRF) due to its inherent thermal and noise insulation functions [1]. Nevertheless, a growing number of literature has highlighted that MIWs may substantially enhance both the stiffness and lateral strength of buildings, consequently altering their dynamic properties [2]. On one hand, neglecting MIWs in structural design can lead to a serious underestimation of seismic demands, thereby compromising the adequacy of the design. On the other hand, the additional strength and hysteretic energy dissipation behavior provided by MIWs can significantly improve the seismic resilience of SMRFs [3]. Hence, a deeper investigation is warranted to elucidate the dualistic role of MIWs in the seismic performance of SMRFs.

Previous studies have explored the influence of MIWs on SMRFs from various perspectives, including static behavior, deterministic modeling, and probabilistic performance [4–6]. Among those probabilistic studies, seismic loadings were always the underappreciated factor. In most cases, the ground motion sets suggested by FEMA P695 [7] were adopted by most scholars [8], or alternatively, records were selected to align with a target design spectrum defined by a

specific intensity measure (IM). These records are subsequently scaled across multiple hazard levels for incremental dynamic analysis (IDA). However, it is important to note that ground motions at varying intensities possess inherently different characteristics—high-intensity records, for instance, are generally accompanied by prolonged durations [9]. As such, a robust probabilistic seismic hazard analysis (PSHA) is essential to capture the full spectrum of seismic sources, intensity levels, and site-specific ground motion scenarios, while rigorously accounting for uncertainties in seismic source characterization, ground motion prediction models (GMPMs), and the target design spectrum. Such a framework ensures that seismic evaluations are both robust and reflective of actual site-specific hazard conditions.

In this study, the seismic fragility analysis of SMRF considering the influence of MIWs is carried out based on a comprehensive PSHA. This paper is organized as follows: Section 2 introduces the methodology of seismic fragility assessment, PSHA, and structural modeling. Section 3 presents the results of seismic disaggregation and ground motion selection, followed by the structural response and fragility analysis derived from nonlinear time-history analysis (NLTHA). In the end, Section 4 summarizes the concluding remarks of the present study.

2 METHODOLOGY

2.1 Seismic fragility assessment

The performance-based seismic assessment developed by Pacific Earthquake Engineering Research center includes four key components: probabilistic seismic hazard analysis (PSHA), probabilistic seismic demand analysis, probabilistic seismic damage analysis and Probabilistic seismic loss analysis [10]. The derivation of fragility function through NLTHA represents a pivotal stage in evaluating seismic performance. Fragility functions are typically characterized by lognormal cumulative distributions, as expressed in Equation (1).

$$P\left(F\left|IM=x\right.\right)=\Phi\left(\frac{\ln\left(x/\theta\right)}{\beta}\right) \tag{1}$$

where $P(F|IM=x)$ is the probability of ground motions with IM will cause failure to occur; $\Phi(\ )$ is the gaussian cumulative distribution function, θ and β are the median and logarithmic standard deviation of the fragility function, respectively.

In this study, multiply stripe analysis method is employed to analysis structural performance at each hazard level. To estimate the parameters θ and β, the maximum likelihood estimation method proposed by Baker [11] is adopted.

2.2 Probabilistic seismic hazard analysis

PSHA quantifies the likelihood of different IM levels of ground shaking occurring at a site, considering all possible earthquake sources and their uncertainties. The ground motions consistent to those hazard conditions are selected and scaled for the further structural analysis. The hazard curve, one of the fundamental output of PSHA, can be calculated by equation (2).

$$\lambda\left(IM>im\right)=\sum_{i=1}^{n_{rup}}P\left(IM>im\left|rup_i,site\right.\right)\lambda\left(rup_i\right) \tag{2}$$

where the $\lambda(IM>im)$ donates the annual occurrence rate of ground motions with IM greater than im; $P(IM>im \mid rup_i, site)$ is the conditional probability of exceeding current IM level for

the given site and i^{th} rupture (rup_i), which can be calculated from the GMPM; $\lambda(rup_i)$ represents the probability of exceedance for the seismic event happening from rup_i.

The PSHA calculation includes seismic source identification, seismic disaggregation, hazard curves development, targeting seismic spectrums calculation, and ground motions selection. The spectral acceleration with 5% damping ratio at the fundamental period of the targeting structure, $Sa(T_1)$, is adopted as the IM. The sixth generation seismic source model of Canada [12] is employed to identify the potential seismic ruptures. The generation of seismic disaggregation and hazard curves are executed by OpenQuake Engine [13].

Following the acquisition the seismic disaggregation results, site-specific target spectrums are developed for each tectonic type. To incorporate the variability of seismic sources and the dynamic properties of the structure, the condition mean spectrum (CMS) [14] is adopted as the target spectrum. The CMS is computed using equation (3).

$$\mu_{\ln Sa(T_i)\left|\ln Sa(T^*)\right.} = \mu_{\ln Sa}\left(M_j, R_j, T_i\right) + \rho\left(T^*, T_i\right)\varepsilon\left(T^*\right)\sigma_{\ln Sa}\left(T_i\right) \tag{3}$$

where T^* is the conditioned period, typically taken the fundamental period of the target structure; $\mu_{\ln Sa(T_i)\left|\ln Sa(T^*)\right.}$ donates the conditional mean spectral acceleration at T_i condition on T^*; $\mu_{\ln Sa}\left(M_j, R_j, T_i\right)$ and $\sigma_{\ln Sa}\left(T_i\right)$ are the mean and standard deviation of logarithmic spectral acceleration at T_i, which can be obtained from GMPM [12]; $\rho\left(T^*, T_i\right)$ is the inter-period correlation coefficient between periods [15,16].

Subsequently, the conditional spectrum (CS)-based probabilistic ground motion selection procedure [17] is utilized in selecting ground motion catering for different ruptures, tectonic types, and structures. The selected ground motion sets are designed to match the target CMS mean and variance, thereby providing a high trustworthiness ground motion set that considers the variability in seismic events.

2.3 Structural modeling

To evaluate the effect of the MIW in SMRFs, a 4-story SMRF buildings are designed in accordance with Nation Building Code of Canada [18] and Canadian Standards S16:24 [19]. A symmetric rectangular plan view was adopted, as shown in Figure 1. The design-related information of SMRF and MIW are presented in Table 1. The same structural design is used for both SMRF and SMRF-MIW systems, with the only difference being the inclusion of MIWs in the latter.

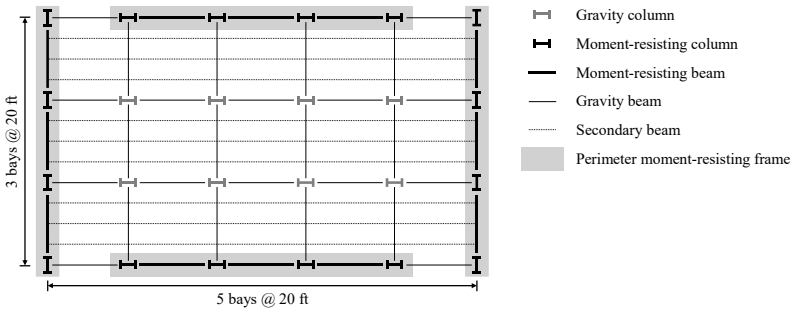

Figure 1: Plan view of architype buildings

Table 1: Design-related information of SMRF and MIW

Type	Parameter	Value
SMRF	Construction location	City Hall, Vancouver, BC, Canada
	V_{s30}	450 m/s
	Frame type	Type-D moment-resisting frame
	Story height	13 ft (15 ft for first floor)
	Steel material	ASTM A992 Gr. 50
MIW	Prism elastic modulus	1980 MPa
	Prism strength	1.9 MPa
	Panel thickness	125 mm
	Infill configuration	Fully infilled in SMRF

Two-dimensional (2D) models of both bare SMRF and infilled SMRF-MIW systems were developed by Python version of Open System for Earthquake Engineering Simulation (OpenSeesPy) [20]. The numerical model of 4-story SMRF and SMRF-MIW system are presented in Figure 2 as an example. The SMRF consists of two major components: the moment-resisting frame, which captures the nonlinear lateral-force-resisting behavior, and an equivalent gravity frame, which accounts for the P-Δ effects as described in [21]. Beams and columns within the moment-resisting frame are modelled by concentrated plasticity methods and *IMK* material [22,23]. The nonlinear behavior of panel zone areas is also considered using a rectangular configuration with a rotational spring modelled by *Hysteretic* material [24].

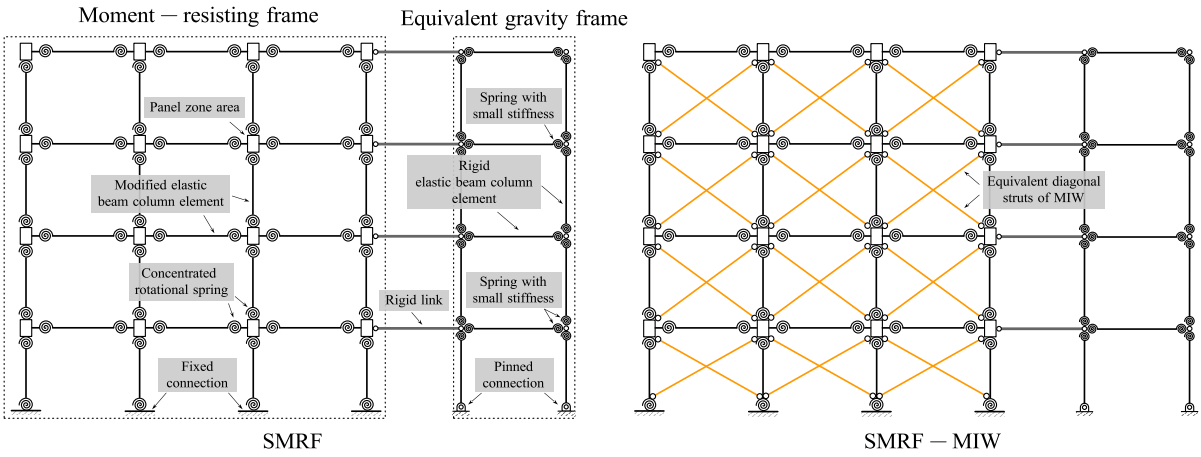

Figure 2: 2D numerical models of SMRF and SMRF-MIW systems

In SMRF-MIW system, the equivalent diagonal struts method is utilized to model the behavior of MIWs. The compression only *Pinching4* material is assigned to struts, whose parameters are derived following the methodology outlined in [25].

3 RESULTS

3.1 Probabilistic seismic hazard analysis results

To accurately capture the influence of site-specific seismicity and ground motion characteristics, PSHA is performed separately for SMRF and SMRF-MIW systems at each hazard level. The fundamental periods of SMRF and SMRF-MIW are 0.99s and 0.49s respectively. Thus, a total of 30 PSHA computations are conducted for two systems at 15 hazard levels with probability of exceeding (PoE) ranging from 0.001% to 40% in 50 years. This comprehensive analysis facilitates the understanding of ground motion composition—particularly in terms of tectonic source types—and supports the selection of ground motions tailored to both seismic hazard and structural characteristics.

The seismic disaggregation results for SMRF and SMRF-MIW systems at selected hazard levels are shown in Figure 3. The corresponding seismic disaggregation properties are presented in Table 2.

In Figure 3 and Table 2, the contribution from different tectonic types determines the number of ground motions belonging to the corresponding tectonic type in the ground motion selection process. The mean magnitude and source-to-site distance of different tectonic types serve as critical inputs to the GMPM, thereby influencing the generation of CMSs. By tailoring both the ground motion combinations and their respective CMSs to the disaggregation outputs, the selected ground motion sets accurately reflect the site-specific seismicity and structural characteristics of the target design.

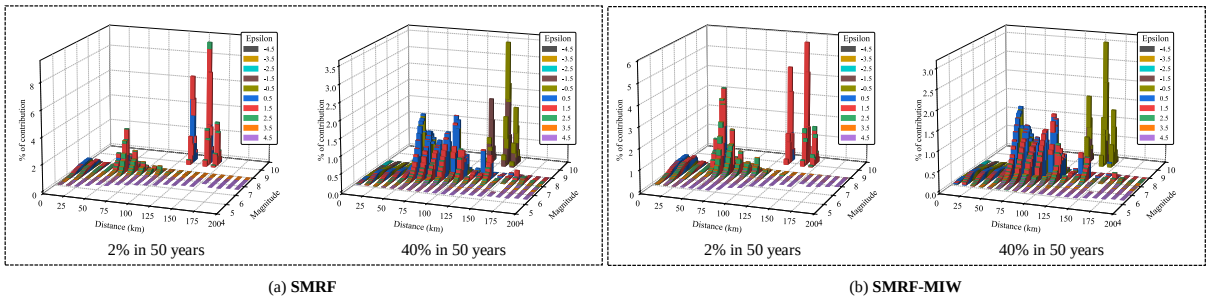

(a) **SMRF** (b) **SMRF-MIW**

Figure 3: Seismic disaggregation results of (a) SMRF system and (b) SMRF-MIW system

Table 2: Contribution, mean magnitude and distance results by seismic disaggregation for 4-story buildings

Building	PoE (%)	Tectonic Type								
		Active Shallow Crust			Subduction Interface			Subduction IntraSlab		
		Contrib. (%)	Mag.	Dist. (km)	Contrib. (%)	Mag.	Dist. (km)	Contrib. (%)	Mag.	Dist. (km)
SMRF	2.0	16.58	6.61	67.26	53.09	8.81	132.29	30.33	6.68	91.52
	40.0	21.24	6.33	82.84	19.48	8.78	132.67	58.97	6.24	103.28
SMRF-MIW	2.0	20.26	6.55	65.33	34.01	8.80	133.21	45.73	6.58	91.28
	40.0	19.92	6.31	82.95	17.01	8.84	130.00	62.84	6.17	103.96

By adopting the abovementioned information, CMSs can be generated by using equation (3). The resulting CMSs for 4-story SMRF and SMRF-MIW systems at parts of hazard levels are presented in Figure 4.

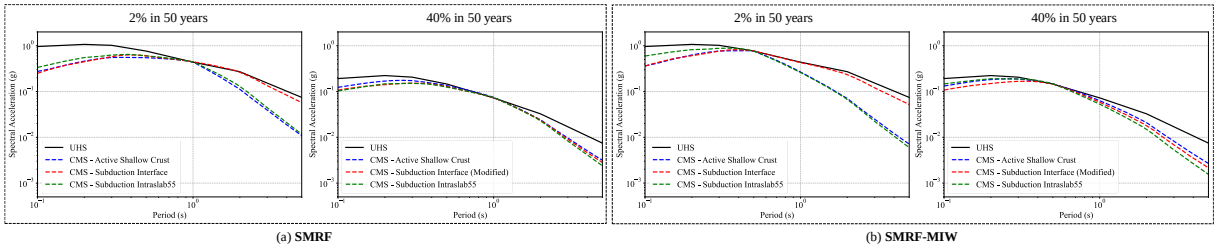

(a) **SMRF** (b) **SMRF-MIW**

Figure 4: CMSs of (a) SMRF system and (b) SMRF-MIW system

To sufficiently consider the record-to-record uncertainty in ground motion sets, 50 ground motions are selected for each building and hazard level. The number of ground motions for different tectonic types is proportional to the respective contributions from the disaggregation analysis. Specifically, the ground motions belonging to the active shallow crust type are selected from NGA West2 database [26], while those representing subduction interface and intraslab events are selected from NGA Subduction database [27]. The ground motion selection results for SMRF system at selected hazard levels are given in Figure 5.

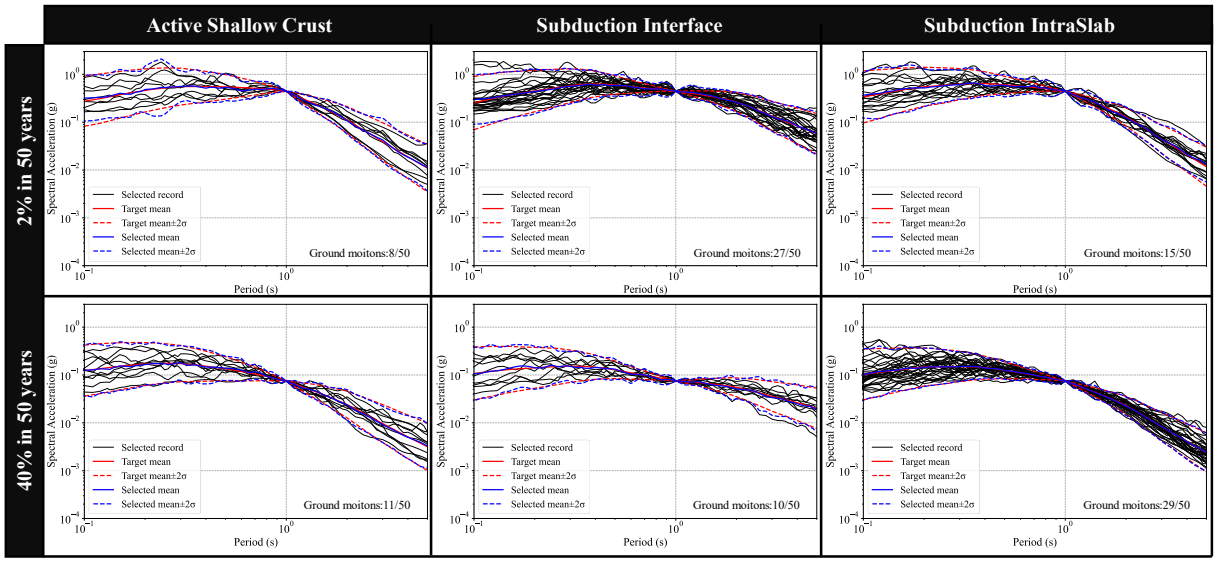

Figure 5: Ground motion selection results for SMRF system

In total, 1,500 ground motion records are selected and scaled to match the CS for the corresponding hazard levels and building systems. Those ground motion records will further be used in the structural analysis.

3.2 Seismic structural response of SMRF and SMRF-MIW system

By adopting the ground motion sets selected from PSHA, 1,500 NLTHAs are conducted for SMRF and SMRF-MIW systems at 15 hazard levels. The maximum IDR results of two systems are presented in Figure 6, where the scatters and the distribution indicate the maximum IDR amount all stories in single analysis and calibrated lognormal distribution for each intensity stripe, respectively.

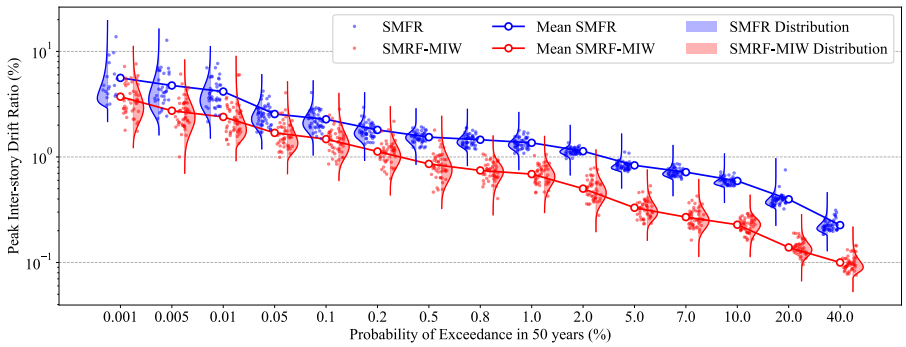

Figure 6: Maximum IDR of SMRF and SMRF-MIW at different hazard levels

It can be seen that the SMRF-MIW systems exhibit substantially reduced IDR responses compared to SMRF systems. The average reduction in IDR amount all hazard levels are 55.3%. Moreover, at high seismic intensities, SMRF-MIW systems exhibit a close performance with SMRF systems, meaning that the MIWs are likely to experience structural failure under strong ground shaking, thereby ceasing to provide any significant beneficial contribution.

3.3 Seismic fragility analysis

To quantify the seismic vulnerability of the structures, fragility analyses are performed for three key performance levels—Immediate Occupancy (IO), Life Safety (LS), and Collapse Prevention (CP)—as defined in FEMA 356 [28] These levels are associated with specific IDR thresholds and corresponding damage descriptions, as summarized in Table 3.

An adaptive analysis strategy is employed during NLTHA to manage convergence difficulties, including step size reduction, increased iteration limits, algorithm switching, and the use of higher-order solvers. Analyses that fail to converge due to excessive IDRs or residual drifts are classified as failures and incorporated into the fragility evaluation. By calibrating equation (1), fragility curves at three performance levels are shown in Figure 7. Vertical dashed lines in the figure denote the spectral accelerations corresponding to Serviceability Earthquake (SE), Design-Based Earthquake (DBE), and Maximum Considered Earthquake (MCE).

Table 3: Structural limit states and damages

Performance Level	IDR (%)	Damage
Immediate occupancy (IO)	0.7	Minor yielding and buckling at few places
Life safety (LS)	2.5	Hinges formed; local buckling of beam can be observed
Collapse prevention (CP)	5.0	Extensive distortion of beam and column panel; many fractures at moment connections

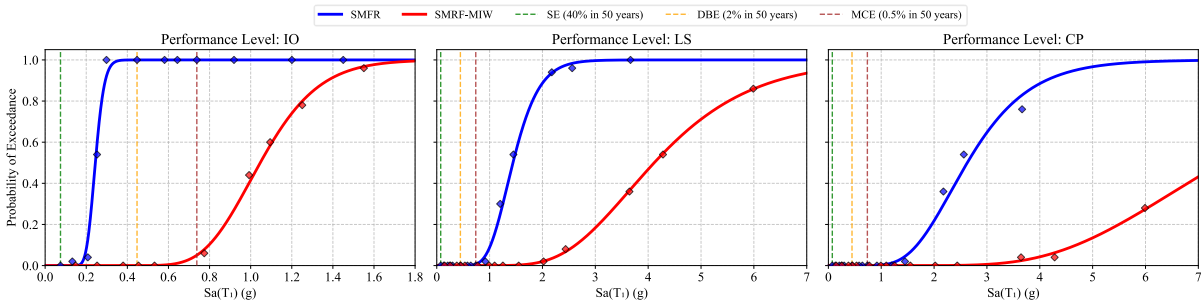

Figure 7: Fragility curves of SMRF and SMRF-MIW at different performance levels

In Figure 7, results clearly demonstrate the beneficial effect of MIWs on structural fragility. Notably, at the IO level, the SMRF-MIW system retains functionality even under MCE, whereas the SMRF system exhibits a near-certain probability of failure. In summary, the inclusion of MIWs significantly enhances the seismic fragility performance across all three performance levels, effectively mitigating damage and reducing collapse potential.

4 CONCLUSIONS

This study evaluates the seismic fragility analysis of steel moment-resisting frames (SMRFs), with and without considering the contribution from masonry infill walls (MIWs). Through a comprehensive probability seismic hazard analysis (PSHA), ground motion sets which are selected consistent to the design site, building properties, and hazard levels. Subsequently, detailed numerical models of SMRF and SMRF-MIW systems are developed in OpenSeesPy. Next, to form fragility functions, nonlinear history analyzes are conducted to get the structural demand at different hazard levels. Fragility curves for two systems are derived and compared at three performance levels. The following conclusion can be drawn:

(1) The PSHA results enable the selection of ground motion sets at different hazard levels that accurately represent site-specific seismic conditions and structural design parameters, thereby ensuring realistic and reliable seismic loading.

(2) The multiple stripe analysis results reveal that, under equivalent hazard levels, additional stiffness, strength, and hysteretic energy dissipation provided by MIWs significantly reduce the seismic response of 4-story SMRF.

(3) With the inclusion of MIWs, SMRF demonstrates a near-zero probability of exceeding the Immediate Occupancy limit state, contrasted to the near-certain exceedance observed in bare SMRFs. Across all performance levels, SMRF with MIWs consistently exhibit lower probabilities of failure.

In conclusion, the presence of MIWs substantially enhances the seismic performance of steel moment-resisting frames by improving stiffness, reducing deformation demands, and delaying the onset of damage for low-rise SMRFs. Their inclusion not only mitigates structural vulnerabilities but also contributes to greater resilience and safety under earthquake loading, underscoring the importance of accounting for infill wall effects in seismic design and assessment. However, further research is needed to evaluate the seismic performance of mid- and high-rise buildings or buildings with varying infill configurations and masonry materials.

REFERENCES

[1] Chelapramkandy R, Ghosh J, Freddi F. Influence of masonry infills on seismic performan ce of BRB-retrofitted low-ductile RC frames. Earthquake Engineering & Structural Dyna mics 2025;54:295–318. https://doi.org/10.1002/eqe.4255.

[2] Beiraghi H. Fundamental period of masonry infilled moment-resisting steel frame buildin gs. The Structural Design of Tall and Special Buildings 2017;26:e1342. https://doi.org/10. 1002/tal.1342.

[3] Dai K, Sun T, Liu Y, Li T, Xu J, Bezabeh MA. Seismic performance of RC frames with s elf-centering precast post-tensioned connections considering the effect of infill walls. Soil Dyn Earthq Eng 2023;171:107969. https://doi.org/10.1016/j.soildyn.2023.107969.

[4] Nicoletti V, Tentella L, Carbonari S, Gara F. Stiffness contribution and damage index of i nfills in steel frames considering moderate earthquake-induced damage. Structures 2024;6 9:107581. https://doi.org/10.1016/j.istruc.2024.107581.

[5] Kazemi F, Asgarkhani N, Jankowski R. Enhancing seismic performance of steel buildings having semi-rigid connection with infill masonry walls considering soil type effects. Soil Dynamics and Earthquake Engineering 2024;177:108396. https://doi.org/10.1016/j.soildy n.2023.108396.

[6] Di Sarno L, Wu J-R. Seismic assessment of existing steel frames with masonry infills. J C onstr Steel Res 2020;169:106040. https://doi.org/10.1016/j.jcsr.2020.106040.

[7] FEMA P 695, others. Quantification of building seismic performance factors. Washington, DC; 2009.

[8] Kazemi F, Asgarkhani N, Jankowski R. Probabilistic assessment of SMRFs with infill ma sonry walls incorporating nonlinear soil-structure interaction. Bull Earthquake Eng 2023;2 1:503–34. https://doi.org/10.1007/s10518-022-01547-0.

[9] Baker JW, Allin Cornell C. Spectral shape, epsilon and record selection. Earthquake Engi neering & Structural Dynamics 2006;35:1077–95. https://doi.org/10.1002/eqe.571.

[10] Moehle J, Deierlein GG. A framework methodology for performance-based earthquak e engineering. 13th world conference on earthquake engineering, vol. 679, WCEE Vancou ver; 2004, p. 12.

[11] Baker JW. Efficient Analytical Fragility Function Fitting Using Dynamic Structural A nalysis. Earthq Spectra 2015;31:579–99. https://doi.org/10.1193/021113EQS025M.

[12] Kolaj M, Halchuk SC, Adams J. Sixth Generation seismic hazard model of Canada: fin al input files used to generate the 2020 National Building Code of Canada seismic hazard values 2023. https://doi.org/10.4095/331387.

[13] Pagani M, Monelli D, Weatherill G, Danciu L, Crowley H, Silva V, et al. OpenQuake Engine: An Open Hazard (and Risk) Software for the Global Earthquake Model. Seismolo gical Research Letters 2014;85:692–702. https://doi.org/10.1785/0220130087.

[14] Baker JW. Conditional Mean Spectrum: Tool for Ground-Motion Selection. J Struct E ng 2011;137:322–31. https://doi.org/10.1061/(ASCE)ST.1943-541X.0000215.

[15] Goda K, Atkinson GM. Probabilistic Characterization of Spatially Correlated Respons e Spectra for Earthquakes in Japan. Bulletin of the Seismological Society of America 200 9;99:3003–20. https://doi.org/10.1785/0120090007.

[16] Baker JW, Bradley BA. Intensity Measure Correlations Observed in the NGA-West2 Database, and Dependence of Correlations on Rupture and Site Parameters. Earthquake S pectra 2017;33:145–56. https://doi.org/10.1193/060716eqs095m.
[17] Baker JW, Lee C. An Improved Algorithm for Selecting Ground Motions to Match a C onditional Spectrum. Journal of Earthquake Engineering 2018;22:708–23. https://doi.org/ 10.1080/13632469.2016.1264334.
[18] Canadian Commission on Building and Fire Codes. National Building Code of Canad a: 2020. National Research Council of Canada; 2022. https://doi.org/10.4224/w324-hv93.
[19] CSA Group. CSA S16:24 Design of steel structures 2024.
[20] Zhu M, McKenna F, Scott MH. OpenSeesPy: Python library for the OpenSees finite el ement framework. SoftwareX 2018;7:6–11. https://doi.org/10.1016/j.softx.2017.10.009.
[21] Elkady A, Lignos DG. Effect of gravity framing on the overstrength and collapse capa city of steel frame buildings with perimeter special moment frames. Earthq Engng Struct Dyn 2015;44:1289–307. https://doi.org/10.1002/eqe.2519.
[22] Lignos DG, Krawinkler H. Deterioration Modeling of Steel Components in Support of Collapse Prediction of Steel Moment Frames under Earthquake Loading. Journal of Struc tural Engineering 2011;137:1291–302. https://doi.org/10.1061/(ASCE)ST.1943-541X.000 0376.
[23] Lignos DG, Hartloper AR, Elkady A, Deierlein GG, Hamburger R. Proposed Updates to the ASCE 41 Nonlinear Modeling Parameters for Wide-Flange Steel Columns in Suppo rt of Performance-Based Seismic Engineering. Journal of Structural Engineering 2019;14 5:04019083. https://doi.org/10.1061/(ASCE)ST.1943-541X.0002353.
[24] Skiadopoulos A, Elkady A, Lignos DG. Proposed Panel Zone Model for Seismic Desi gn of Steel Moment-Resisting Frames. Journal of Structural Engineering 2021;147:04021 006. https://doi.org/10.1061/(ASCE)ST.1943-541X.0002935.
[25] Huang H, Burton HV, Sattar S. Development and Utilization of a Database of Infilled Frame Experiments for Numerical Modeling. Journal of Structural Engineering 2020;146: 04020079. https://doi.org/10.1061/(ASCE)ST.1943-541X.0002608.
[26] Bozorgnia Y, Abrahamson NA, Atik LA, Ancheta TD, Atkinson GM, Baker JW, et al. NGA-West2 Research Project. Earthquake Spectra 2014;30:973–87. https://doi.org/10.11 93/072113EQS209M.
[27] Bozorgnia Y, Abrahamson NA, Ahdi SK, Ancheta TD, Atik LA, Archuleta RJ, et al. N GA-Subduction research program. Earthquake Spectra 2022;38:783–98. https://doi.org/10. 1177/87552930211056081.
[28] FEMA 356 FE, others. Prestandard and commentary for the seismic rehabilitation of b uildings. Federal Emergency Management Agency: Washington, DC, USA 2000.